

Enhancement of Semi-Automated Lineament Extraction from IRS- 1B Satellite Images for Part of Himalayan Region

Pradhan, B.,¹ Pirasteh, S.,² and Varatharajoo, R.,³

¹Institute for Cartography, Faculty of Forestry, Geo and Hydro-Science, Dresden University of Technology 01062 Dresden, Germany, E-mail: Biswajeet.Pradhan@mailbox.tu-dresden.de, biswajeet@mailcity.com

²Institute for Advanced Technologies (ITMA), University Putra Malaysia, 43400, UPM, Serdang, Selangor Darul Ehsan, Malaysia, E-mail: moshaver1380@yahoo.co.uk

³Department of Aerospace Engineering, Faculty of Engineering, University Putra Malaysia, 43400, UPM Serdang, Selangor Darul Ehsan, Malaysia

Abstract

This paper presents the results of a spatial domain filtering investigation of lineament mapping from IRS- 1B LISS- I satellite image. A quick and accurate lineament extraction method is applied to a big IRS-1B scene of the study area. Further, the orientation and structural trend of the area is also discussed with respect to the derived lineaments. Efforts have been made to evaluate the techniques as a fast algorithm for quick and time limited analysis of lineaments from which their orientations are estimated. To achieve the objective, various filtering techniques have been used for extraction of the lineaments from IRS-1B scene. In the present study, the acquired IRS-1B satellite scene after being geocoded, has been divided into twelve equal sized windows and a separate raster layer has been made for each of the windows. Two computer programs were used for preparation of the data sets and plotting of the rose diagrams. The result demonstrated that the lineament density value is relatively higher in the high relief area which indicates the presence of fractured rocks with abundant joints and faults owing to the structurally active terrain. As a conclusion, the current method has been found to be useful for lineament extraction from a complex terrain.

1. Introduction

Over the last decade, lineament extraction using satellite remote sensing data is very common. Lineament maps prepared by conventional field mapping technique cannot identify all the lineaments existing in any area, due to enlarged scale. In the aerial photography survey, a large scale regional lineaments, which extend far beyond the coverage of the photos cannot be detected due to the lack of continuity in the successive photo pairs, therefore they could be detected by means of smaller sub-segments. Digital remote sensing with the availability of multi-spectral and progressive development in the image enhancement techniques is an opportunity to prepare relatively more reliable and comprehensive lineament maps. The wide ground coverage and relative high resolution with respect to scale presented by the satellite images, also enables regional and local lineament analysis. The term lineaments originally proposed by Hobbs (2004) as significant lines of landscape that reveal the hidden architecture of the rock basement. However, O'Leary et al., (1976) defined lineaments as a simple or composite linear feature whose parts are aligned in a rectilinear or slightly curvilinear relationship and which differs from the pattern of

adjacent features that reflects some subsurface phenomenon. There are numerous approaches existing for the evaluation and automatic detection of lineaments and curvilinear features from satellite images (Cross, 1988, Cross and Wadge, 1988, Taud and Parrot, 1992, Hardcastle, 1995, Karnieli et al., 1996, Vasil'yev et al., 1996, Budkewitsch et al., 1994, Waters, 1990, Zakir et al., 1999, Koch and Mather, 1997 and Suzen and Topak, 1998). Image processing of extraction lineament system using different algorithms have been used by various researchers (Ramli et al., 2009 and Dash et al., 2000). Among image enhancement techniques in particularly, the spatial domain filtering is one of the best objective tools for the construction of the segment maps, including the application of digital filters which introduces certain artifacts into the maps. This paper, applies several filtering techniques for the extraction of lineaments for part of the Garhwal Himalayan region. In the present study, IRS-1B LISS-I satellite image have been used to deduce various linear feature information after pre-processing of the data. Figure 1 shows the IRS 1B FCC (4, 2, 1) image around Himalayan region.

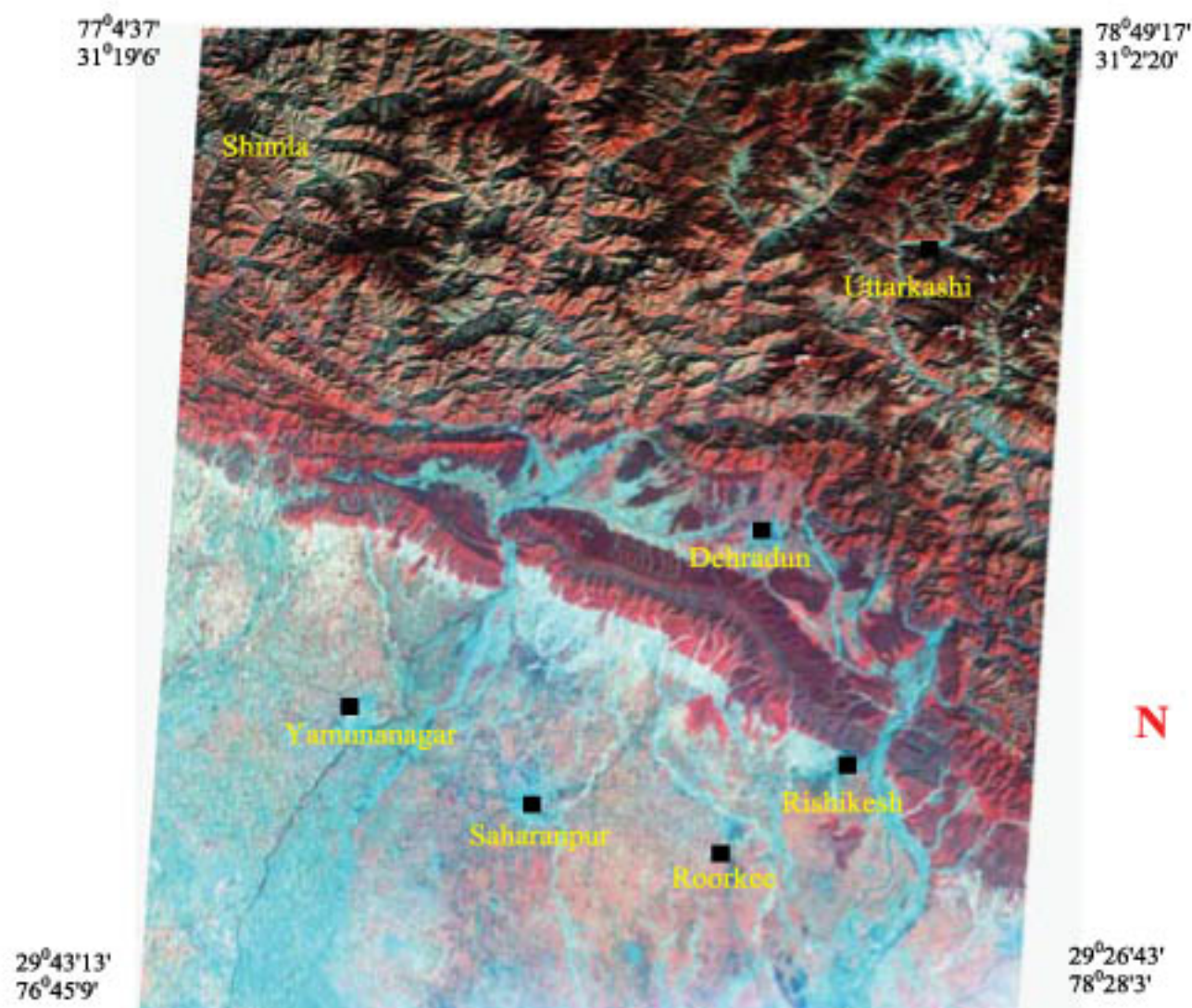


Figure 1: shows the IRS 1B FCC (4, 2, 1) image of the study area

2. Previous Research on Lineament Identifications

Previously, various techniques have been used to enhance lineaments using remote sensing data. The edge detection method may be archived in various ways such as using optical instruments like 'Ronchi Rolling method' and the common used digital image processing. But the digital image processing is more reliable and easier than other methods. A digital spatial filtering technique that is much more efficient than the other processes such as Fast Fourier Transformation (Karnieli et al., 1996 and Richards, 1993). The filter works with data in image space and gives equal weight to every picture elements (pixel) within the filter window or kernel used. But however this process is having some limitations as all the non-geological features are also detected (Philip, 1996). Thus expert human eye and more experience are required in order to delineate the actual linear features on the image. Singh and Singh (2005) used the lineaments analysis to study changes in stress pattern for earthquake analysis in India. They used IRS-1D LISS data for lineament analysis. The lineaments are extracted using high pass filter (Sobel filter in all direction) with high level accuracy. From the thorough examination of the literature it was inferred that, computer assisted

methods for the detection of structural (tectonic) lineaments (namely faults and joints), were exclusively based on spatial filtering techniques (directional or gradient filters) as well as morphological filters (Morris, 1991, Math et al., 1995, Philip, 1996 and Suzen and Topak, 1998). These methods produced edge maps requiring further processing (thresholding and thinning) for the linear segments to appear with one-pixel thickness. Optimal edge detectors (e.g the canny algorithm) have already been successfully applied on natural scenes with quite satisfactory results (binary images with one pixel thickness, efficient length and pixel connectivity), and this makes their application in geologic lineament mapping more popular (Canny, 1986 and Tripathi et al., 2000). In the literature, Hough transform algorithms has been applied successfully in geological research, especially to detect geological lineaments such as fault, joints, dykes, and shear zones. Recently, Fitton and Cox (1998) used multi-scale method to enable detection of smaller features and a novel normalization method to ensure the identification of off-centered features Won et al., (1998) utilized RADARSAT SAR data for a geological lineament study, but they did estimate lineaments via visual investigation of SAR images rather than automatic

lineament extraction approach. Kageyama et al., (2000) used airborne SAR and Landsat 5 TM for lineament extraction.

3. Methodology

The objective of this study is to investigate the contribution of different filtering techniques, particularly spatial domain filtering for the extraction of the lineaments from IRS 1B image. Efforts have been made to evaluate the techniques as a fast algorithm for quick and time limited analyses of linear features from which their orientations are estimated. The study area which is part of the Garhwal Himalaya is characterized by numerous faults with consistently striking in the same direction or even some are cutting across them (Philip, 1996, Sahoo et al., 1998, Shao et al., 2000 and Pradhan et al., 2006). The identification of lineaments has paramount importance in geology, because such features can represent faults and fracture zones where offset has not occurred (Sabins, 1987). These features always play an important role for significant potential hazardous occurrences. A fault may be directly visible in the satellite image as a scarp or change in lithology (Jain, 1987). Thus this goal can be achieved from digital images, through image processing methods by using various edge detecting methods. But however each edge detected in this kind of process is true in some mathematical sense, may be they all are not geologically correct or significant. The present study attempts to extract the lineaments from the IRS 1 B image which has a spatial resolution of 72 m pixel size. Figure 2 shows the methodology applied for the current study.

3.1 Spatial Domain Filtering

As a preliminary step, two dimensional spatial filtering was used to generate images that enhanced both regional and intermediate-level linear features (Jensen, 1996). A spatial filter will generally enhance features that are less than half the size of the kernel being used and suppress features that are more than half the kernel size. The types of filters are selected as directional high pass filters (Süzen and Toprak, 1998), since the major directions of the linear features of the study area are known. The process starts in the rule of thumb knowledge that filtering will also recognize the non-geological lineaments and the location of the lineament will be biased and enlarged dependent on the kernel size (Dash et al., 2000). In the present study, various types of kernels have been used to detect the all possible lineaments:

- Prewitt kernel in all principal directions
- Sobel Operations in all directions
- 11 by 11 low pass and 7 by 7 vertical convolution kernel

3.1.1 Prewitt operator

Prewitt kernels (Table 1) are the first filter group convolved over the image in four principal directions (N-S, NE-SW, E-W, and NW-SE). The filter images are added back to the original band in all equal proportions. However, it has been seen that there is no significant increase in the contrast and frequency relative to the unfiltered original image, thus the output lineament map is very similar to the original image with only minor improvements. For the next step, biased Prewitt, Sobel filters are used to increase the frequency and contrast.

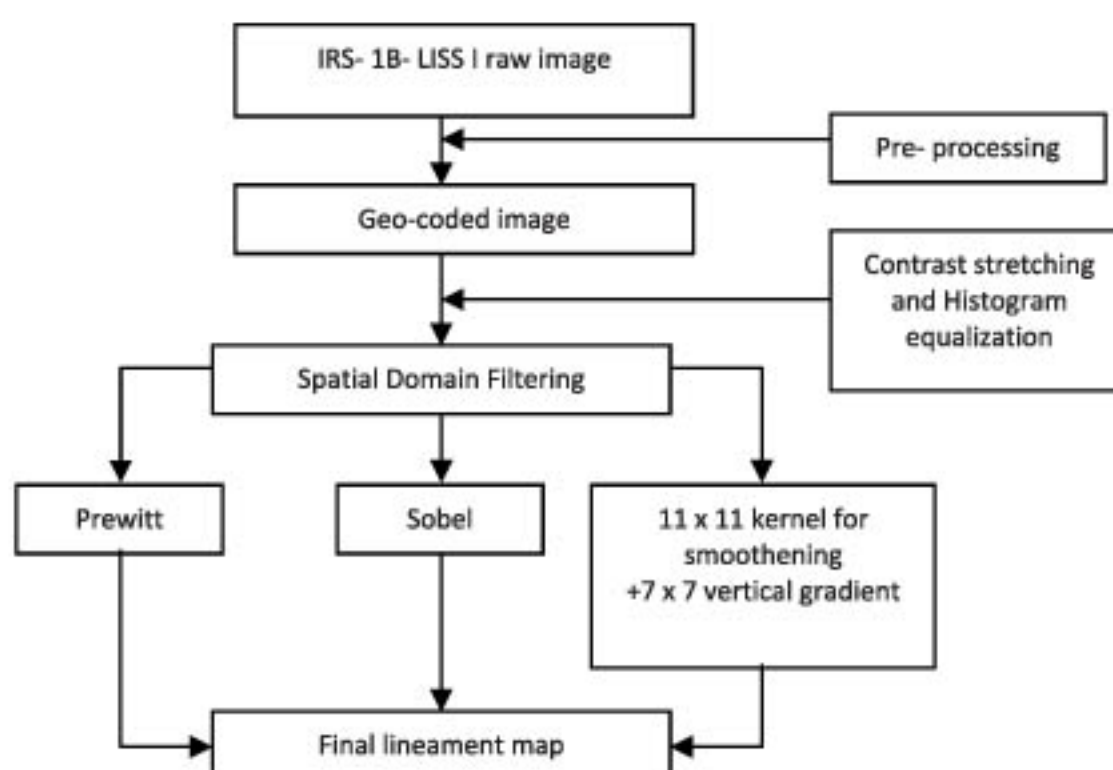


Figure 2: Methodology flowchart for lineament extraction and detection

Table 1: shows the Prewitt and Sobel kernels in four principle directions

	N-S			NE-SW			E-W			NW-SE		
PREWITT	-1	0	1	-1	-1	0	-1	-1	-1	0	1	1
	-1	0	1	-1	0	1	0	0	0	-1	0	1
	-1	0	1	0	1	1	1	1	1	-1	-1	0
SOBEL	-1	0	1	-2	-1	0	-1	-2	-1	0	1	2
	-2	0	2	-1	0	1	0	0	0	-1	0	1
	-1	0	1	0	1	2	1	2	1	-2	-1	0

3.1.2 Sobel operator

It is a non-linear edge enhancement technique that performed using nonlinear combinations of pixels. If the first derivative pixel is above a threshold, the presence of an edge pixel is assumed. It based on the notation of the 3x3 window described and computed according to the relationship (Table 1) (Duda and Hart, 1973 and Gonzalez and Wintz, 1977).

a ₀	a ₁	a ₂
a ₇	[i,j]	a ₃
a ₆	a ₅	a ₄

Consider the arrangement of the pixels about the pixel [i,j]. The Sobel operator is the magnitude of the gradient computed as:

$$M = \sqrt{S_x^2 + S_y^2}$$

Where,

$$S_x = (a_2 + ca_3 + a_4) - (a_0 + ca_7 + a_6)$$

$$S_y = (a_0 + ca_1 + a_2) - (a_6 + ca_5 + a_4)$$

$$c = 2$$

Equation 1

Like the other gradient operators, S_x and S_y can be implemented by using convolution masks:

$$\begin{array}{ccc} 0 & 1 & 1 \\ S_x = -2 & 0 & 2 \\ -1 & 0 & 1 \end{array} \quad \begin{array}{ccc} 2 & 1 & -1 \\ S_y = 0 & 0 & 0 \\ -1 & -2 & -1 \end{array}$$

Equation 2

This is the convolution mask for non-directional Sobel operator and places an emphasis on pixels that are closer to the center of the mask. Sobel kernels can also be convoluted in desired directions. Then it gives on the direction for which it is applied. Sobel kernels (Table 1) are convolved in four principal directions and added back to the original image in equal proportions. It has been seen that the out coming result is more satisfactory than the Prewitt kernels but the lineaments have a segmented appearance, may be due the increased spatial

frequency. It is much more sensitive to segments of lineaments rather than a combined unique lineament. In order to get regional lineaments bigger size convolution kernels are used. In the present study, the whole scene after being geocoded, has been divided into twelve different equal sized windows and each window has been processed separately. Each window has been subjected to both Prewitt and Sobel convolution kernels. Then all the output edge enhanced images have been visually interpreted and the small lineaments have been annotated in another layer. Finally all the individual windows have been joined to its original coordinates and the lineament fabric has also been shown on the original satellite imagery (Figure 3). The lineament fabric has also been subjected to further statistical processing to find length-weighted rose diagrams.

3.1.3 11 x 11 low pass and 7 x 7 vertical gradient filters

Although the original image is added back, due to their small size and to their emboss effect, Sobel and Prewitt filters become much more sensitive to segments of lineaments rather than a combined unique lineament. In order to combine these segments, to get regional lineaments and to reduce the noise present in the image, the image is smoothed by using 11 by 11 low pass filters (Table 2). The effect of smoothening in the image is reflected by homogenization and blurring, giving a decrease in spatial frequency. The effect of smoothening in the image is to reduce any single random lineaments or small lineaments which can easily be assigned to crop boundaries or simply non-geological lineaments. Moreover, homogenization is preferred in fault zones rather than mapping individual lineaments as segments. Thus to enhance the newly found NW-SE lineament set, the previously cited NE-SW set without the interference of smaller random and non-geological lineaments, a bigger size vertical gradient filter (7 x 7) (Table 3) is convolved over the smoothed image and the flirited image is added back to the original one in equal proportions. Finally, all the gathered data from spatial domain enhancements are used to create a final lineament map and the rose diagram by deleting the duplication of the file record.

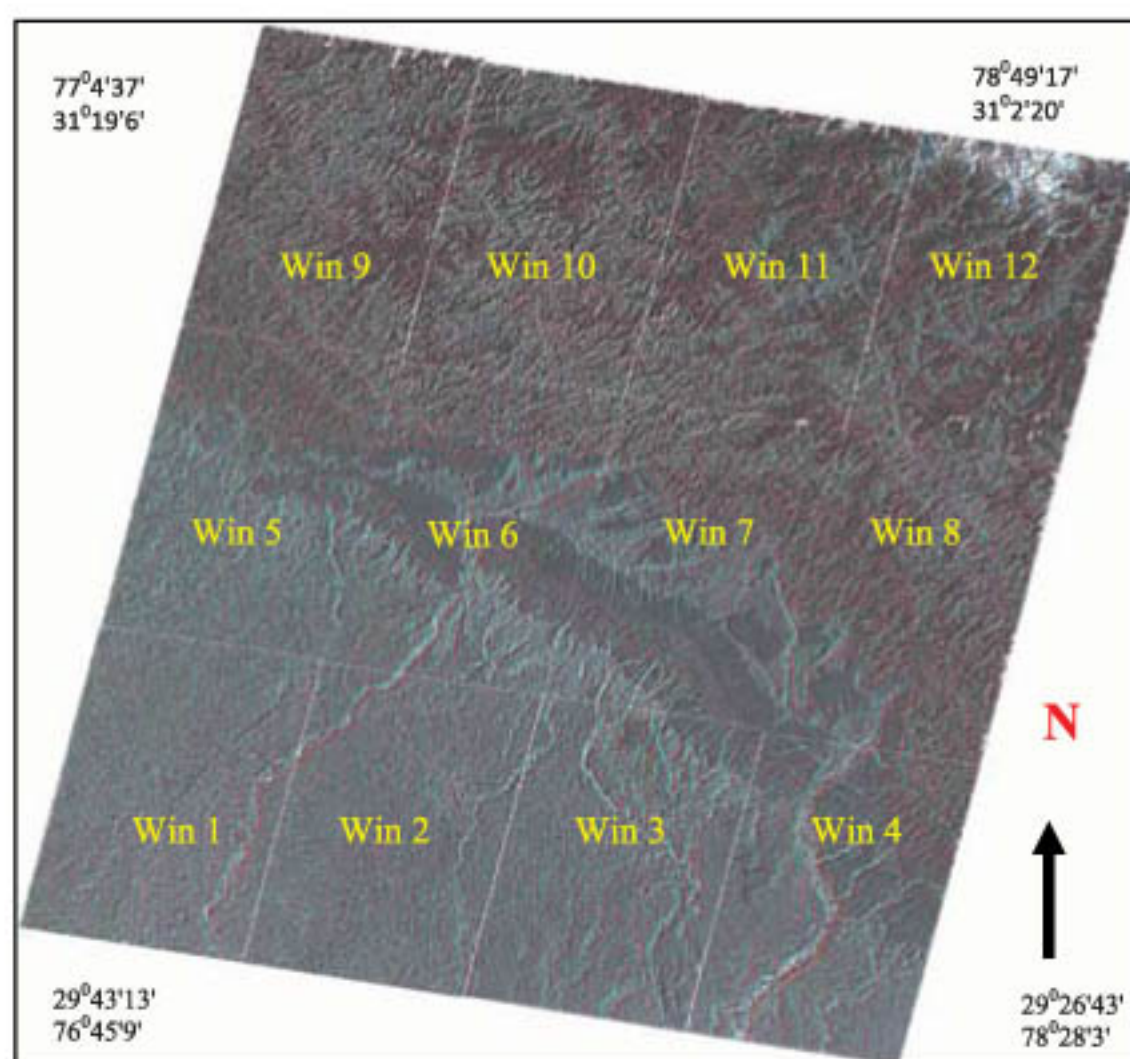


Figure 3: shows the lineament fabric of the study area in different windows overlaid on FCC (4, 2, 1) image

Table 2: 11 by 11 Low Pass kernels convolved over the IRS LISS 1 image

1	1	1	1	1	1	1	1	1	1	1
1	1	1	1	1	1	1	1	1	1	1
1	1	1	1	1	1	1	1	1	1	1
1	1	1	1	1	1	1	1	1	1	1
1	1	1	1	1	1	1	1	1	1	1
1	1	1	1	1	1	1	1	1	1	1
1	1	1	1	1	1	1	1	1	1	1
1	1	1	1	1	1	1	1	1	1	1
1	1	1	1	1	1	1	1	1	1	1
1	1	1	1	1	1	1	1	1	1	1
1	1	1	1	1	1	1	1	1	1	1

Table 3: 7 by 7 Vertical gradient kernels convolved over the IRS LISS 1 image

1	1	1	0	-1	-1	-1
1	2	2	0	-2	-2	-1
2	3	4	0	-4	-3	-2
3	4	5	0	-5	-4	-3
2	3	4	0	-4	-3	-2
1	2	2	0	-2	-2	-1
2	3	4	0	-4	-3	-2

4. Statistical Evaluation of the Lineament Fabric

Data and Construction of Rose Diagrams

In the present study, lineament extraction has been used for the fault line and other fracture lines analysis. To achieve a good visual interpretation, rose diagrams have been plotted for the directional analysis of the lineaments. Rose diagram is a circular histogram used by most geologists to depict the distribution of the directional data. It is plotted between class frequency and length of the lineaments on a 180 degree compass. It certainly

depicts the relative abundance of the data in particular direction, within a given range. After getting the lineament fabric data from each individual window, a separate raster layer has been made for each of the windows. As all the depicted annotated lineament layers in each window are simply the lines, so it was become very necessary to change these lines into polylines for preparation of the raw data. Then all the lineaments in each window are transformed to the polyline and their coordinates were stored. Each line or lineament is

represented in the file with a separate group. The first line of each group has the line ID (identity) and last line with end characters with some more header informations. The intermediate lines show the coordinates in terms of latitude and longitude of the starting and intermediate points in the line. Two computer programs have been used for preparation of the data sets and plotting the rose diagrams. First a computer program has been used to remove the coordinates of all the intermediate points in each line. Hence the final file is only having the data for the first and last points (in terms of coordinates) for each line. The second program has been coded in compatible MATLAB software for plotting of the rose diagrams. The rose diagram has been plotted by taking into the consideration of the length and the frequency of the lineaments for each window. Initially, the length-weighted rose diagram is calculated by simple mathematical formula.

$$\text{length} = \sqrt{(y_2 - y_1)^2 + (x_2 - x_1)^2}$$

Equation 3

Similarly the slope (orientations) of each line has been calculated from the formula:

$$\text{slope} = \frac{y_2 - y_1}{x_2 - x_1}$$

Equation 4

Where; x_1, y_1 and x_2, y_2 are the coordinates of the initial and final points of the lineaments. Finally slope of each lineament has been calculated by above mentioned procedure and grouped into classes for a particular class interval of 10° range. Similar procedures have been followed for all the 12 windows, and rose diagrams have been plotted. Figure 4 shows the rose diagram for the length weighted lineament fabric in all windows, and Figure 5 shows the rose diagram for the frequency count lineament fabric in all windows. The results reported here can be compared with the findings of Sahoo et al., (2000) who used IRS 1B imagery in a study of stress measurement of the same area though his test areas do not overlap with the present study area.

5. Results and Discussion

Due to spatial domain filtering, smoothing effect of the image can be explained by low pass filters. The homogenization and smoothing of the image, reduces the segmented appearance of the lineaments. Due to smoothing effect, all the desegmented lineaments fused together to give single continuous lineaments Figure 6). As the chosen IRS- 1B image was taken when the solar illumination direction was SE, taking into consideration of the shadow conditions a vertical gradient filter could also be chosen but the major E-W striking regional lineaments would mask the remaining areas.

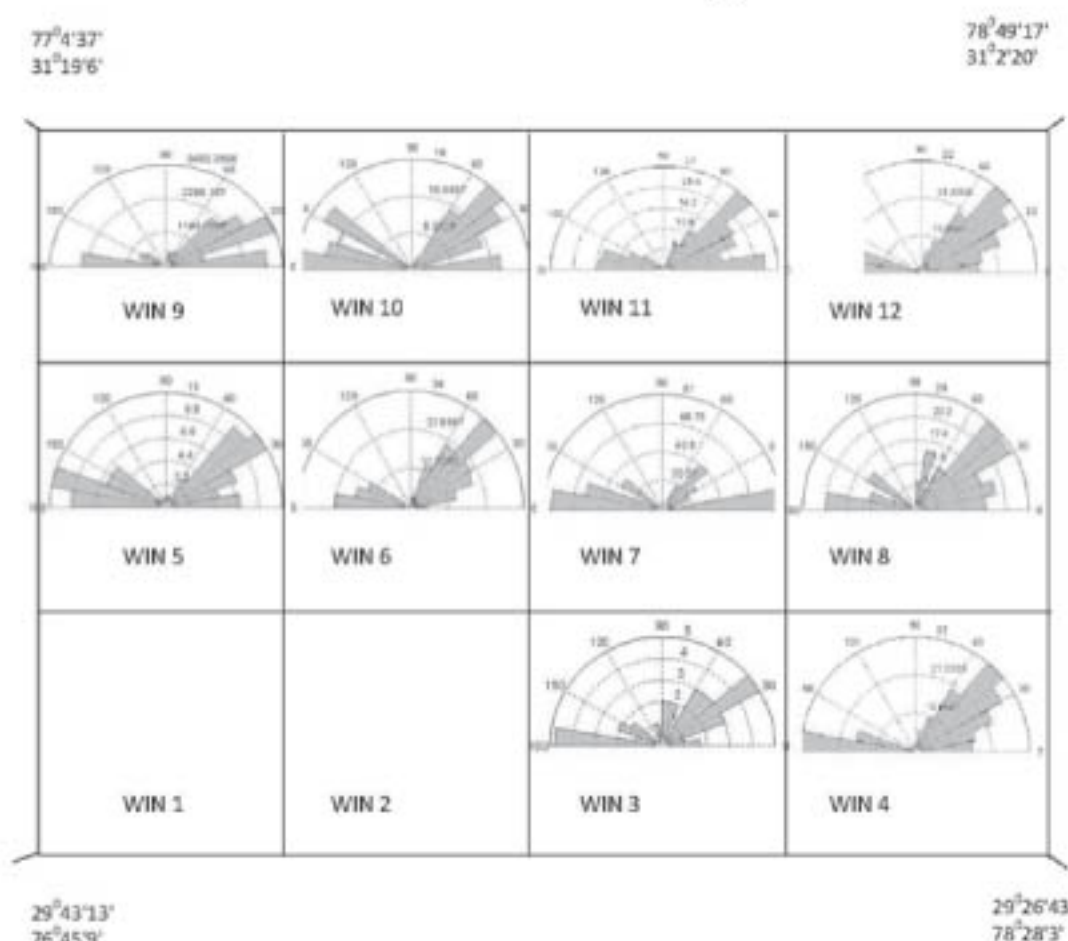


Figure 4: shows the rose diagrams showing the frequency of lineaments per 10 degree interval in different windows of the IRS scene

77°4'37"
31°19'6"

78°49'17"
31°2'20"

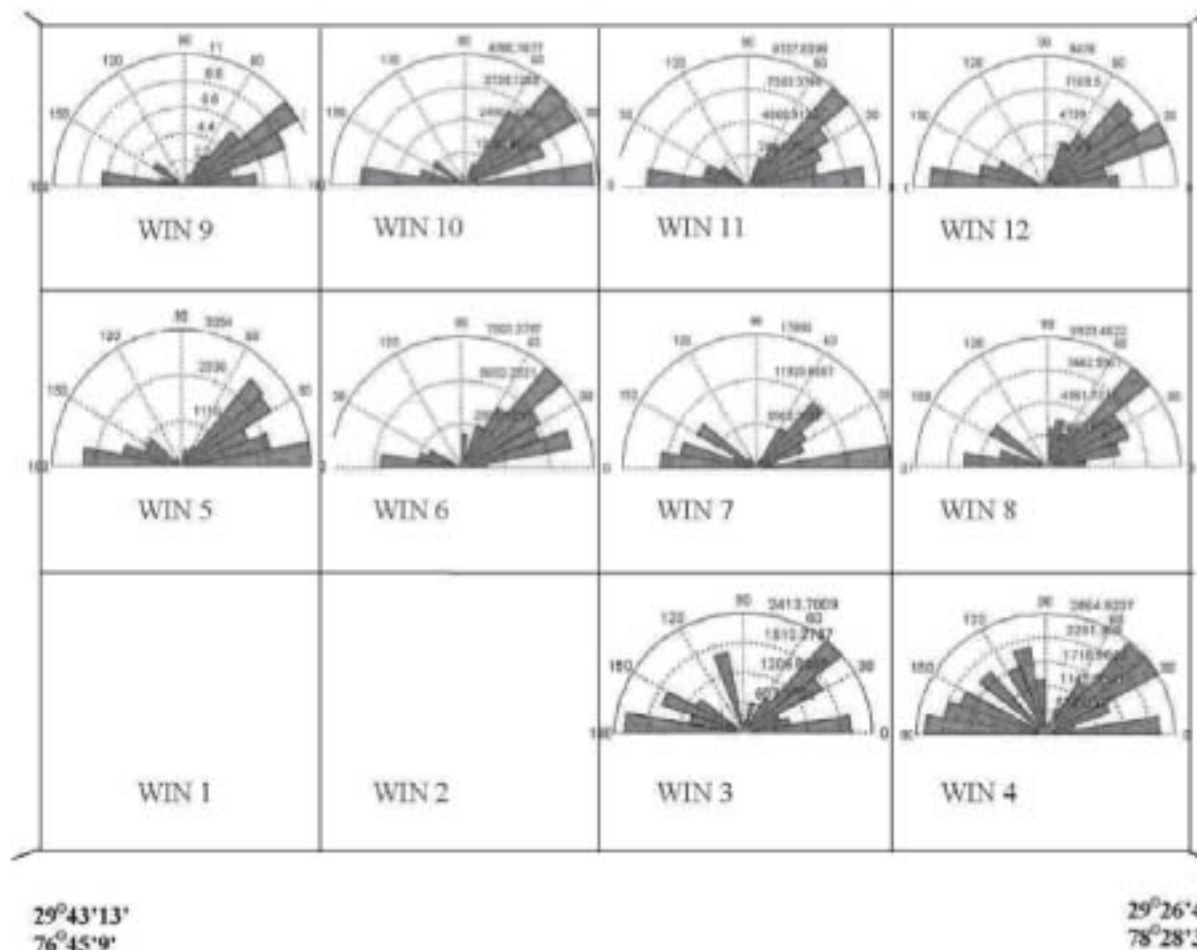


Figure 5: shows the rose diagrams showing the cumulative length of lineaments per 10 degree interval in different windows of the IRS scene



Figure 6: shows the screen shot of the window 12 after convolution of 11 by 11 and 7 by 7 vertical filter

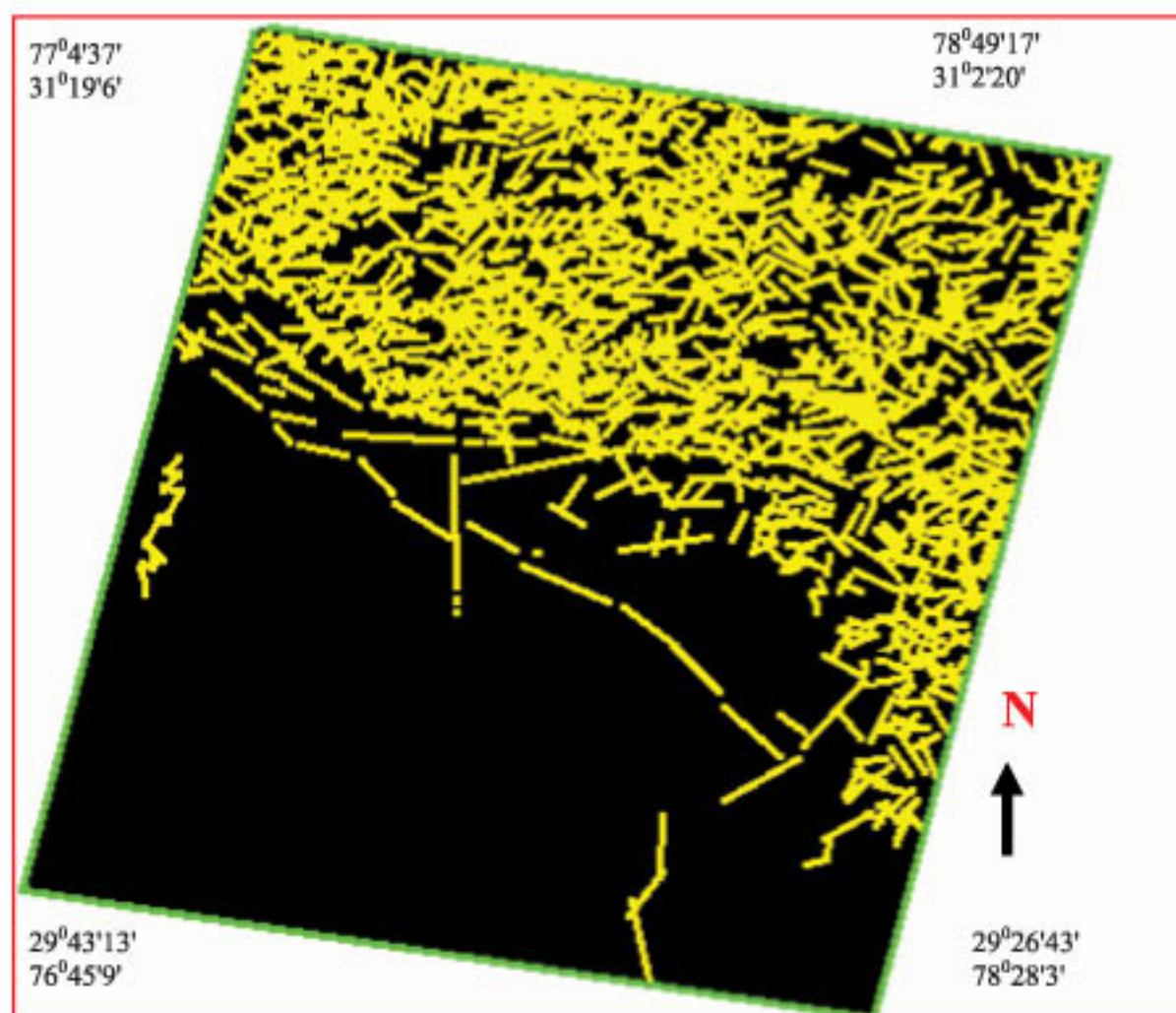


Figure 7: shows the final lineament map of the study area based on IRS image scene

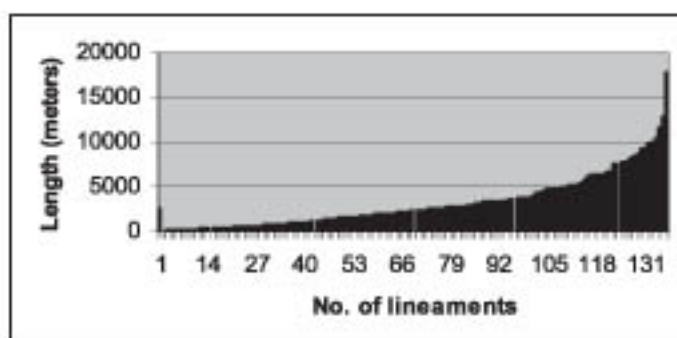


Figure 8: shows the frequency histograms of lengths of lineaments derived from IRS scene

79 percentages of the total detected lineaments shows NE trend by indicating that Himalayan plate is facing in NE direction. Though the size of the image is relatively big with 72.5 m spatial resolution, the current analysis clearly shows out that it is the quick process in comparison with the large size of the data. Manual way of detecting the lineaments in this case is extremely difficult and so also the edge enhancement technique would not be very much useful. An enormous number of lineaments were observed in the chosen IRS scene, including a number of major lineaments crossing the area. The lineaments occur as anomalous straight river courses and valleys, as well as anomalous straight features crossing hills and mountain ranges, sometimes marked by a clear lateral displacement of rocks on both side of the lineament. It is evident that

these major lineaments represent fault and fracture zones (Figure 7). Their numbers and total lengths were expressed in meters. Rose diagram of lineament fabric reveals that there is distinct change in major trend of lineaments in north and south of MBT (Figure 7). In the lesser Himalayan region, maximum number of lineaments are oriented in east-west direction. In the Dun region, the trend of lineaments are found to be in the direction of E-W and in the Siwalik region the majority trend of the lineaments are directed towards in the NE- SW direction. Figure 8 shows the frequency histograms of length of lineaments derived from the image for a comparative analysis.

6. Conclusions

The detection of long, linear features was successfully operated by using the current method. Lineament analysis of a selected IRS scene was carried out by using various image processing techniques. A total number of 1508 lineaments were detected by using the current technique. Considering the time schedule and the minimum budget various enhancement techniques were applied on original satellite data. Due to the directional characters of applied Prewett and Sobel filters are sensitive to lineaments oriented parallel or sub-parallel to the kernel. In the output lineament map the major peak is observed within the range of N60°E to N30°E, which is the main structural orientation of the area.

But, however, the presence of E-W and N-W lineaments in the rose diagram indicate the slight changes in the orientation of the study area in four directions.

Acknowledgements

Thanks to the two anonymous reviewers for their valuable comments which helped to bring the manuscript to the current form.

References

- Budkewitsch, P., Newton, G., and Hynes, A. J., 1994, Characterization and Extraction of Linear Features from Digital Images. *Canadian Journal of Remote Sensing*, Vol. 20, 268-279.
- Canny, J. F., 1986, A Computational Approach to Edge Detection. *IEEE Transactions on Pat. Anal. and Mach. Int.*, Vol. 8, 679-714.
- Cross, A., and Wadge, G., 1988, Geological Lineament Detection using the Hough Transform, *Proceedings of the IGRASS 88 Symposium*, Edinburgh, Scotland, 13-16 Sept. 1988, (Paris: ESA Publications Division), 1779-1782.
- Cross, A. M., 1988, Detection of Circular Geologic Features using the Hough Transform. *International Journal of Remote Sensing*, Vol. 9, 1519-1528.
- Dash, P., Singh, R. P., and Voss, F., 2000, Anomalous Stress Pattern in Chamoli Region Observed from IRS-1B Data. *Current Science*, Vol. 78(9), 1066-1070.
- Duda, R. O., and Hart, P. E., 1973, *Pattern Classification and Scene Analysis*. Wiley-Interscience, USA, 2nd Edition.
- Fitton, N. C., and Cox, S. J. D., 1998, Optimising the Application of the Hough Transform for Automatic Feature Extraction from Geoscientific Images, *Computers & Geosciences*, Vol. 24, No. 10, 933-951.
- Gonzalez, R. C., and Winz, P., 1977, *Digital Image Processing*. Addison-Wesley, Massachusetts.
- Hardcastle, K., 1995, Photo-Lineament Factor: A New Computer-Aided Method for Remotely Sensing the Degree to which the Bed Rock is Fractured. *Photogrammetric Engineering and Remote Sensing*, Vol. 61, 739-747.
- Hobbs, W. H., 2004, Lineaments of the Atlantic Border Region. *Geological Society American Bulletin*, 15: 483-506.
- Jain, A. K., 1987, Kinematics of the Transverse Lineaments Regional Tectonics and Holocene Stress Field in the Garhwal Himalaya. *Journal Geological Society of India*, Vol. 30, 169-186.
- Jensen, J. R., 1996, *Introductory Digital Image Processing, A Remote Sensing Perspective*, 2nd edition (New Jersey: Prentice Hall).
- Kageyama, Y., Nishida, M., and Oi, T., 2000, Analysis of the Segments Extracted by Automated Lineament Detection, *Proceeding of IGARSS 2000, Geoscience and Remote Sensing Symposium*, Vol. 1, 289-291.
- Karnieli, A., Meiseis, A., Fisher, L., and Arkin, Y., 1996, Automation Extraction of Geological Linear Features from Digital Remote Sensing Data using Hough Transform. *Photogrammetric Engineering and Remote Sensing*, Vol. 62, 525-531.
- Koch, M., and Mather, P. M., 1997, Lineament Mapping for Groundwater Resource Assessment: A Comparison of Digital Synthetic Aperture Radar (SAR) Imagery and Stereoscopic Large Format Camera (LFC) Photographs in the Red Sea Hills, Sudan. *International Journal of Remote Sensing*, Vol. 18, No. 7, 1465-1482.
- Math, A., Taylor, G. R., Lennox, P., and Balia, L., 1995, Lineament Analysis of Landsat TM Images, Northern Territory, Australia. *Photogrammetric Engineering and Remote Sensing*, Vol. 61, 761-773.
- Morris, K. 1991, Using Knowledge-Base Rules to Map the Three-Dimensional Nature of Geological Features. *Photogrammetric Engineering and Remote Sensing*, Vol. 57, 1209-1216.
- O'Leary, D. W., Friedman, J. D., and Pohn, H. A., 1976, Lineaments, Linear, Lineations: Some Proposed New Standards for Old Terms, *Geol. Soc. Am. Bull.*, Vol. 87, 1463-1469.
- Philip, G., 1996, Landsat Thematic Mapper Data Analysis for Quaternary Tectonics in Parts of Doon Valley, NW Himalaya, India. *International Journal of Remote Sensing*, Vol. 17, 143-153.
- Pradhan, B., Singh, R. P., and Buchroithner, M. F., 2006, Estimation of Stress and its use in Evaluation of Landslide Prone Regions using Remote Sensing Data. *Advances in Space Research*. Vol. 37, 698-709.
- Ramli, M. F., Yusof, N., Yusoff, N. K., Juahir, H., and Shafri, H. Z. M., 2009, Lineament Mapping and Its Application in Landslide Hazard Assessment: A Review. *Bull Eng Geol Environ.* (article on-line first available). DOI 10.1007/s10064-009-0255-5
- Richards, J. A., 1993, *An Introduction to Remote Sensing Digital Image Analysis*, Springer-Verlag, Berlin.

- Sabins, F. F., 1987, Remote Sensing Principles and Interpretation (Second edition), W.H. Freeman and Company, New York.
- Sahoo, P. K., Kumar, S., and Singh, R. P., 1998, Estimation of Tectonic Stress in NW Himalaya region using IRS-1B data. *Current Science*, Vol. 74, 780- 786.
- Sahoo, P. K., Kumar, S., and Singh, R. P., 2000, Neotectonic Study of Ganga and Yamuna Tear Faults, NW Himalaya, using Remote Sensing and GIS. *International Journal of Remote Sensing*, Vol. 21, 499- 518.
- Singh, V. P., and Singh, R. P., 2005, Changes in Stress Pattern Around Epicentral Region of Bhuj Earthquake, *Geophysics Research Letter* 32 (2005) 10.1029/2005GL023912.
- Süzen, M. L., and Toprak, V., 1998, Filtering of Satellite Images in Geological Lineament Analyses; An Application to a Fault Zone in Central Turkey. *International Journal of Remote Sensing*, Vol. 19, No.6, 1101-1114.
- Taud, H., and Parrot, J. F., 1992, Detection of Circular Structures on Satellite Images. *International Journal of Remote Sensing*, Vol. 33, 319- 335.
- Tripathi, N. K., Gokhale, K. V. G., and Siddiqui, M. U., 2000, Directional Morphological Image Transforms for Lineament Extraction From Remotely Sensed Images. *International Journal of Remote Sensing*. Vol. 21, 3281-3292.
- Vasil'yev, L. N., Kachalin, A. B., Moralev, V. M., Terekhov, Y. N., and Tyuflin, A. S., 1996, The Multifractal Character of Lineament Density on the Kola Peninsula. *Mapping Science and Remote Sensing*, Vol. 33, 135- 143.
- Waters, P., 1990, Methodology of Lineament Analysis for Hydrogeological Investigations. In *Satellite Remote Sensing for Hydrology and Water Management* edited by E. C. Barret, C. H. Power, and A. Micallef (New York: Gordon & Breach), 1-23.
- Won, J. S., Ryu, J. H., and Chi, K. H., 1998, RADARSAT SAR Investigation of Lineament and Spring Water in Cheju Island, *Journal of Korean Society of Remote Sensing*, Vol. 14, No. 4, 325-342.
- Zakir, F. A., Qari, M. H. T., and Mostafa, M. E., 1999, A New Optimising Technique for Preparing Lineament Density Maps. *International Journal of Remote Sensing*, Vol. 20, No.6, 1073-1085.